SNI
SURGICAL NEUROLOGY INTERNATIONAL
OPEN ACCESS
For entire Editorial Board visit : http://www.surgicalneurologyint.com
Editor: James I. Ausman, MD, PhD University of California, Los Angeles, CA, USA

Original Article

Biocompatibility of reduced graphene oxide nanoscaffolds following acute spinal cord injury in rats

Ali H. Palejwala[1,5], Jared S. Fridley[1,5], Javier A. Mata[1,5], Errol L. G. Samuel[6], Thomas G. Luerssen[1,5], Laszlo Perlaky[2,8], Thomas A. Kent[3,4,9], James M. Tour[6,7], Andrew Jea[1,5]

Departments of [1]Neurosurgery, [2]Pediatrics, [3]Neurology, and [4]Interdepartmental Program in Translational Biology and Molecular Medicine, Baylor College of Medicine, [5]Division of Pediatric Neurosurgery, Texas Children's Hospital, Houston, Departments of [6]Chemistry, [7]Chemistry and Materials Science and NanoEngineering, Rice University, [8]Research and Tissue Support Services Core Laboratory, Texas Children's Cancer and Hematology Services, [9]Center for Translational Research in Inflammatory Diseases, Michael E. DeBakey VA Medical Center, Houston, Texas, USA

E-mail: Ali H. Palejwala - ali.palejwala@bcm.edu; Jared S. Fridley - fridley@bcm.edu; Javier A. Mata - jmatans@gmail.com; Errol L. G. Samuel - errol.l.samuel@rice.edu; Thomas G. Luerssen - tgluerss@texaschildrens.org; Laszlo Perlaky - lxperlak@texaschildrens.org; Thomas A. Kent - tkent@bcm.edu; James M. Tour - tour@rice.edu; *Andrew Jea - ahjea@texaschildrens.org
*Corresponding author

Received: 29 April 16 Accepted: 20 June 16 Published: 23 August 16

Abstract

Background: Graphene has unique electrical, physical, and chemical properties that may have great potential as a bioscaffold for neuronal regeneration after spinal cord injury. These nanoscaffolds have previously been shown to be biocompatible *in vitro*; in the present study, we wished to evaluate its biocompatibility in an *in vivo* spinal cord injury model.

Methods: Graphene nanoscaffolds were prepared by the mild chemical reduction of graphene oxide. Twenty Wistar rats (19 male and 1 female) underwent hemispinal cord transection at approximately the T2 level. To bridge the lesion, graphene nanoscaffolds with a hydrogel were implanted immediately after spinal cord transection. Control animals were treated with hydrogel matrix alone. Histologic evaluation was performed 3 months after the spinal cord transection to assess *in vivo* biocompatibility of graphene and to measure the ingrowth of tissue elements adjacent to the graphene nanoscaffold.

Results: The graphene nanoscaffolds adhered well to the spinal cord tissue. There was no area of pseudocyst around the scaffolds suggestive of cytotoxicity. Instead, histological evaluation showed an ingrowth of connective tissue elements, blood vessels, neurofilaments, and Schwann cells around the graphene nanoscaffolds.

Conclusions: Graphene is a nanomaterial that is biocompatible with neurons and may have significant biomedical application. It may provide a scaffold for the ingrowth of regenerating axons after spinal cord injury.

Key Words: Biocompatibility, cytotoxicity, graphene, nanomedicine, neuron, spinal cord injury

Access this article online
Website: www.surgicalneurologyint.com
DOI: 10.4103/2152-7806.188905
Quick Response Code:

How to cite this article: Palejwala AH, Fridley JS, Mata JA, Samuel EL, Luerssen TG, Perlaky L, *et al*. Biocompatibility of reduced graphene oxide nanoscaffolds following acute spinal cord injury in rats. Surg Neurol Int 2016;7:75.
http://surgicalneurologyint.com/Biocompatibility-of-reduced-graphene-oxide-nanoscaffolds-following-acute-spinal-cord-injury-in-rats/

INTRODUCTION

Few options are available for the treatment of spinal cord injury (SCI), despite years of research on the subject. Supportive medical care and early surgical decompression, when applicable,[19] remain the cornerstones of management following acute injury.[60] SCI can be divided into primary and secondary injury.[8-11,19,60] Primary SCI refers to the initial insult to the spinal cord. It includes a heterogeneous group of mechanisms such as contusion/compression, stretch injury, and transection of various degrees. These injuries can lead to axonal disruption and tissue degeneration.[19,60]

A consequence of SCI is the formation of scar tissue and posttraumatic microcystic myelomalacia.[28] The extent of each of these post-injury maladies depends on injury severity. Two types of scar tissue can be formed, namely, glial and fibrous.[3,4,14,15,17,18,23,25,26,29,30,32,33,36,39,51,52,59,61] The glial scar consists of a loose network of astrocytic processes connected by tight junctions.[7] There has recently been a challenge to a prevailing dogma that glial scars are regarded as a failure of axonal regrowth in the central nervous system. Instead, astrocytes in SCI lesions were found to express multiple axon-growth-supporting molecules responsible for stimulating axonal regrowth past scar-forming astrocytes.[5] Fibrous scarring is made up of extracellular matrix deposition and type IV collagen, which form a tight barrier. In addition to creating a mechanical barrier, both types of scars may obstruct neuronal regeneration. Current tissue engineering research is focused on constructing a permissive environment at the site of injury that would support axonal regeneration.[3,4,14,15,17,18,23,25-27,29,30,32,33,36,39,51,52,59,61]

Development of a bioscaffold that assists with neural tissue regeneration and the prevention/bypass of scar formation is an ongoing area of research. Graphene, a two-dimensional (2D) sheet of sp^2-hybridized graphitic carbon,[2,45] is a substance of recent interest in neurosurgery, one of the applications of which is as a SCI bioscaffold because the following unique properties give graphene tremendous biomedical potential: Zero-gap semiconductor characteristics,[13,44] high thermal conductivity,[6,21] high surface area-to-volume ratio,[22] and chemical modifiability, which allows for functionalization of biotherapeutic molecules.[37] Most studies on graphene have focused on novel uses in electrical transport and composite materials, with little focus on biological applications, excluding nascent investigations in biosensing.[24,43,55,62-64] Thus, the bioapplicability and potential cytotoxic effects of graphene rarely have been studied. Two recent noteworthy studies have examined the cytotoxic effects of graphene and graphene oxide (GO) in solution on pheochromocytoma-derived PC12 cells. Solubilized graphene, however, does not mimic the needs for growth surfaces.[1,69]

Two-dimensional graphene films have been used for studying neuronal growth *in vitro*,[48] however, they do not translate well to *in vivo* applications. As a result, we searched for a new three-dimensional (3D) graphene-based material that could be used as a scaffold *in vivo*. Recent efforts have demonstrated the production of self-assembled 3D hydrogels by reducing GO using a variety of conditions.[16,35,50,57,58,65,68] Because these reduced graphene hydrogels exhibit excellent mechanical strength and high electrical conductivity, they may be more relevant to biomedical applications in the regeneration of acutely and chronically injured spinal cords.[48] Studying structured graphene with neurons is of further importance when considering that multiple studies have documented that electrically inducible alignment of neural cells and growth of axons yield clinical improvement in patients with SCI.[47,49,53]

Given graphene's potential as a nanoscaffold that might physically support, electrically stimulate, positionally inform, and organize the 3D cytoarchitecture required for axonal regeneration, there is a need to assess the interaction and bioreactivity of this nanomaterial with mammalian neuronal cells in a rat model for SCI. At this early phase of our investigation of graphene as an adequate scaffold in the setting of SCI, we are not ready to compare our nanoscaffold with that of other authors.[3,4,14,15,17,18,23,25,26,29,30,32,33,36,39,51,52,59,61] The novelty of our study lies in the use of graphene in an *in vivo* model of SCI. To the best of our knowledge, the biocompatibility and use of reduced graphene has not been investigated previously.

MATERIALS AND METHODS

Graphene oxide scaffold preparation

GO (38 mg, produced by the method of Marcano *et al*.[41]) was dissolved in 10 mL of deionized water in a glass test tube with the aid of sonication. $NaHSO_3$ (75 mg) was added, and the mixture was vortexed briefly. The tube was heated at 90°C for 16 to 20 h and then cooled to room temperature. The resulting hydrogel was removed from the tube and stored in deionized water in a 20 mL scintillation vial before use.

The morphology of the resulting hydrogel was characterized by scanning electron microscopy (SEM) after lyophilization. The porous structure was formed by crosslinking graphene sheets. The pore sizes ranged from hundreds of nanometers to several micrometers [Figure 1].

Scaffold implantation and animal care

A hemispinal cord transection was selected as a model for evaluating *in vivo* the effect of graphene implantation on SCI immediately after creating the lesion. Twenty (19 male, 1 female) 8-week-old Wistar rats (Velaz, Ltd., Prague, Czech Republic), each weighing 300–400 g, were used. Eight hours prior to the surgery, food was withheld,

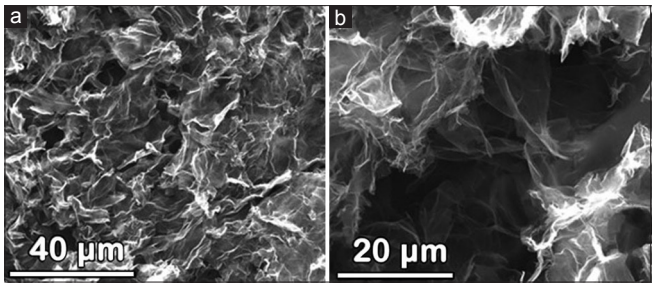

Figure 1: Scanning electron microscopic images of lyophilized graphene gels with (a) bar = 40 μm and (b) bar = 20 μm. Based on the images, the pore sizes range from hundreds of nanometers to several micrometers

and carprofen (analgesic tablets) was administered. Anesthesia was induced by means of inhaled 2% isofluorane. The skin over the upper thoracic spine was shaved and prepped. A laminectomy was performed at approximately T2 under a surgical microscope using aseptic technique. The dura was opened; a 2 mm-wide hemi-segment of spinal cord was excised from the left side, producing the SCI. The segment was examined using a surgical microscope to ensure that no remaining tissue was left.

In 10 animals, a hydrogel matrix (HydroGel™, Portland, Maine) was laid onto the injured spinal cord and open dura. This was followed by approximation of paraspinal muscle with sutures (Vicryl, Johnson and Johnson, Somerville, New Jersey) and skin closure with skin staples (MultiFire Premium, Covidien, Dublin, Ireland). These animals served as the control group.

In 10 animals, we inserted an approximately 2 × 2 × 2-mm block of the reduced GO scaffold with an overlying layer of hydrogel matrix. This was followed by muscle and skin closure. These animals served as the treatment group.

In both groups, bladder expression was performed until recovery of sphincter control; enrofloxacin (5–10 mg/kg) was administered subcutaneously for 7 days to prevent urinary infection. Animals were kept in cages with food and water *ad lib*. Pain control was provided for 5 days after surgery with buprenorphine (0.05–0.5 mg/kg), banamine (2–4 mg/kg), and/or rimadyl tablets. This study was performed in accordance with the guidelines of our Institutional Animal Care and Use Committee (IACUC) and was approved by the Baylor College of Medicine Institutional Review Board (Protocol #AN-6016).

No unexpected deaths occurred in follow-up before intentional sacrifice of the animals in the present experimental protocol. In prior study iterations with a complete transection of the spinal cord, we had experienced an unacceptably high mortality rate secondary to permanent bladder dysfunction and presumed urinary tract infection/urosepsis.

Tissue processing and histology

The animals were sacrificed 3 months after the surgery using CO_2 inhalation. A 3 cm-long segment of the thoracic spinal column with spinal cord (including injury epicenter with implanted graphene scaffold and/or hydrogel) was carefully dissected out and left overnight in 10% buffered neutral pH formalin. The bone was removed; the spinal cord itself was postfixed in the same fixative for 24 h. Each spinal cord was embedded in paraffin and cut in the coronal plane into 10 μm-thick sections on a cryostat. The sections were stained with Hematoxylin and eosin (H and E), Luxol fast blue, and cresyl violet using standard protocols. For immunohistochemical studies, the following primary antibodies and dilutions were used: GFAP-Cy3 (1:200, Sigma-Aldrich, St. Louis, Missouri) to identify astrocytes, NF 160 (1:200, Sigma-Aldrich, St. Louis, Missouri) to identify neurofilaments, p75 (1:100, Chemicon International, Temecula, California) to identify Schwann cells, RECA-1 (1:50, Abcam, Cambridge) to identify endothelial cells of blood vessels, ED-1 (1:100, Invitrogen, Waltham, Massachusetts) to identify macrophages, CS-56 (1:50, Sigma-Aldrich, St. Louis, Missouri) to identify chondroitin sulfate, and CD4 (1:800, Abcam, Cambridge, UK). Alexa Fluor 488 goat anti-rabbit IgG (1:200, Invitrogen, Waltham, Massachusetts), IgM Cy3 (1:100, Chemicon International, Temecula, California), and Alexa Fluor 594 goat anti-rabbit IgG (1:500, Invitrogen, Waltham, Massachusetts) were used as secondary antibodies. To confirm the presence of cells, immunostained sections were additionally stained with DAPI (0.4 ug/ml, Chemicon International, Temecula, California) to identify all the cell nuclei.

The authors acknowledge financial support from the U.S. Army Telemedicine Advanced Technology Research Center (TATRC)/Alliance for NanoHealth (Grant No. W81XWH-09-2-0139; A.J. and J.M.T.); AOSpine North America Young Investigator Research Award (A.J.) and Texas Children's Hospital Department of Surgery Seed Research Fund (A.J.). For the remaining authors, none was received.

RESULTS

Comparison of control and treatment groups

We compared the results of reduced GO hydrogel scaffold implantation in the treated group with the hydrogel-only implantation control group. The treatment group showed good graphene scaffold integration inside the lesion site [Figure 2]. No pseudocyst cavities were found at the implant-tissue borders. The mechanical properties of the scaffold appeared to allow it to adhere to the spinal cord stumps; it did so without applying excessive pressure, as evidenced by the lack of structural distortion of the

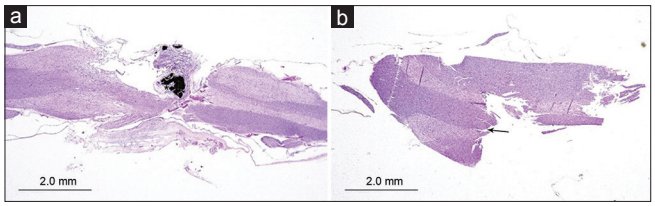

Figure 2: Representative photomicrographs showing spinal cord injury development after hemispinal cord transection at the T2 level (a) with reduced graphene oxide nanoscaffold performed immediately after transection and (b) without nanoscaffold implantation (control group). Notice the area devoid of tissue (*arrow*) at the lesion site in the control slide, suggesting possible pseudocyst formation. By contrast, cell proliferation (*asterisk*) is exuberant with implantation of the nanoscaffold, and no cavity is evident. Hematoxylin and eosin bar = 2 mm

surrounding nervous tissue. Rats treated with hydrogel matrix alone developed large areas devoid of tissue at the lesion site after injury, suggesting possible pseudocyst formation [Figure 2].

Histological evaluation of reduced graphene oxide scaffold integration

Three months after SCI, connective tissue elements, such as fibroblasts, collagen, blood vessels, and chondroitin sulfate, were densely adherent in and around the graphene nanoscaffold [Figure 3]. Cellular infiltration close to the nanoscaffold consisted mostly of macrophages, as seen on H and E-stained sections and confirmed with ED-1 immunohistochemical studies, together with a few CD4-positive lymphocytes. Histologically, we searched for any inflammatory response or adverse reaction of the tissue to the implanted material. Except for occasional foreign body granulomas seen at the implant-tissue borders, no purulent inflammatory reaction was observed.

Neurofilaments grew toward the nanoscaffold at the tissue-implant border [Figure 3]. Schwann cells (p75-positive cells) were also noted at the lesion site. They readily adhered to the graphene nanoscaffold. Outside of the hydrogel, most p75-positive cells were found at the spinal root zone, the most probable source of these Schwann cells. Astrocytes, the predominant cell type in glial scar formation, seemed to be inhibited from proliferation at the spinal cord-implant border [Figure 3].

DISCUSSION

Histologic observation of the lesion site in the hydrogel-only matrix showed a large area devoid of tissue [Figure 2]. Pseudocyst cavities, which commonly form in areas of necrotic tissue following SCI, most likely occupied this space before preparation of the slide. This formation creates an environment that is an inhibitory influence for tissue regeneration. These negative histological findings have been confirmed in other studies.[3,4,14,15,17,18,23,25-27,29,30,32,33,36,39,51,52,59,61]

Tissue engineering and nanotechnology represent a promising approach for modulating the perilesional inhibitory environment in SCI to facilitate recovery and axonal growth. Other authors have used a variety of biomaterials and nanoparticles in SCI as an injectable nonstructured delivery vehicle after injury, with or without seeding with neural stem cells. Promising materials for scaffolds have included natural polymers, such as collagen, agarose, chitosan, and synthetic polymers such as poly(lactide-co-glycolide)/polyethylene glycol.[3,4,14,15,17,18,23,25,26,29,30,32,33,36,39,51,52,59,61] An optimal scaffold should provide mechanical support and a suitable environment for cell adhesion and growth.

Collagen, a widely used biomaterial, is both biocompatible and biodegradable.[3,25,26,30,52] In one study, completely transected spinal cord stumps of rats were bridged by collagen tubes. Results showed aligned axon growth within the tube lumen and a reduction in the density of glial scar formation.[52,54] In a rabbit SCI model, aligned collagen filaments were grafted into the rabbit spinal cord with a 3-mm defect. Axons regenerated across the distal and proximal ends of the implants. Improved functional recovery in the locomotor rating scale was observed in the grafted group compared with the nontreated control group.[52,67]

Agarose, a biocompatible material that can withstand biodegradation over a month *in vivo*,[32,52] can be fabricated as a scaffold with guidance pores. The scaffolds are stable under physiological conditions without the need for crosslinking.[52,56] Agarose scaffolds containing a brain-derived neurotrophic factor (BDNF) have been used to treat completely transected spinal cord and have shown significant axonal regeneration.[20,52] In one study, freeze-dried agarose scaffolds with uniaxial channels were implanted into an injured rat spinal cord.[52,56] This study showed that the agarose scaffolds were well integrated into the host tissue, and aligned axonal growth was seen in the scaffolds 1 month after the surgery.

Chitosan is a naturally available polysaccharide found in the exoskeletons of crustaceans and insects. After being filled with type I collagen, a chitosan tube was implanted in a transected spinal cord.[29,34,52] Regenerated axons connected the distal and proximal ends of the lesion site, leading to functional recovery, as indicated by Basso, Beattie, and Bresnahan evaluation. The study suggested that chitosan, in combination with collagen, can potentially block glial scar tissue formation and facilitate the directional projection of axons.[34]

Poly(lactic-co-glycolic acid) (PLGA), a synthetic copolymer of polylactic acid and polyglycolic acid, is biocompatible and biodegradable.[36] The degradation rate of the copolymer can be controlled by altering the ratio of polylactic acid and polyglycolic acid.[40] Neural

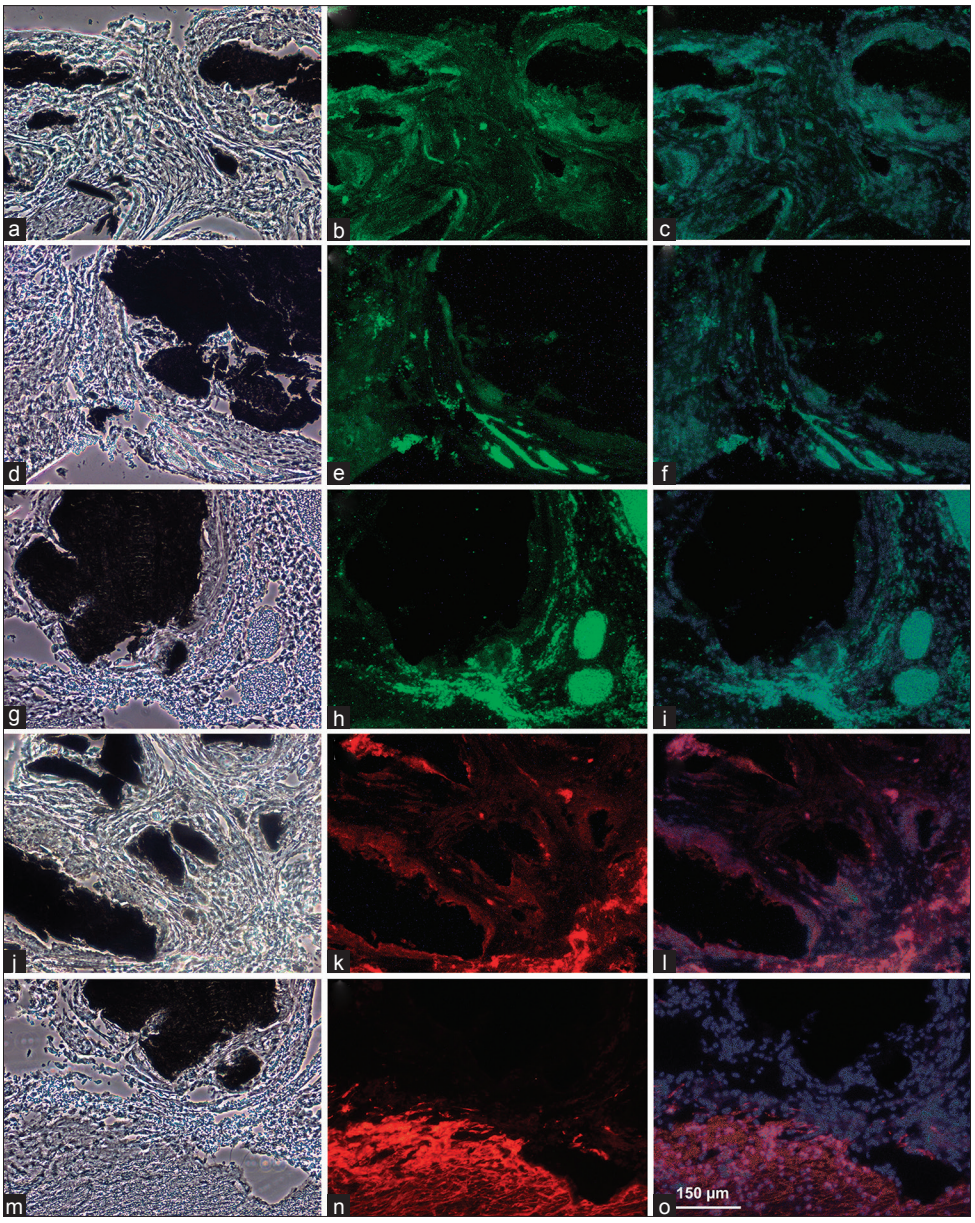

Figure 3: Photomicrographs. CS-56 demonstrates chondroitin sulfate around the nanoscaffold: (a) Phase contrast, (b) immunostained, and (c) DAPI superimposed. RECA-1 demonstrates the presence of blood vessels: (d) Phase contrast, (e) immunostained, and (f) DAPI superimposed. NF-160-g488 shows neurofilaments: (g) Phase contrast, (h) immunostained, and (i) DAPI superimposed. P75 shows Schwann cells: (j) Phase contrast, (k) immunostained, and (l) DAPI superimposed. GFAP-Cy3 demonstrates astrocytes: (m), Phase contrast, (n) immunostained, and (o) DAPI superimposed. Bar = 150 µm

conduits fabricated from PLGA have been implanted into completely transected rat spinal cord. Axonal regeneration was observed in the channels of the neural conduits.[42,46] However, it was noted that the breakdown of PLGA produced glycolic and lactic acids, which lowered the local pH and could hinder the tissue-repair process.

The graphene nanoscaffold, when implanted into the site of injury, provided a surface for growth, attachment, and survival of tissue [Figure 2]. Similar to PEG and chitosan, the graphene nanoscaffold may represent a substance with the power to fuse together severed axons and seal injured leaky neurons in the GEMINI spinal cord fusion protocol.[12,31,66] The regenerating tissue migrated into the lesion site toward the graphene nanoscaffold and then demonstrated the ability to incorporate itself onto the surface of the implant. By examining the cytoarchitecture under phase-contrast microscopy, we were able to further characterize this growth. There was an ingrowth of tissue into the graphene nanoscaffold, with strong attachment at the implant-tissue border [Figure 4] and robust growth of tissue around these graphene nanoscaffolds [Figure 4].

We were able to confirm neuronal regeneration with NF-160-stained slides, which demonstrated neurofilament growth that paralleled the contour of the graphene

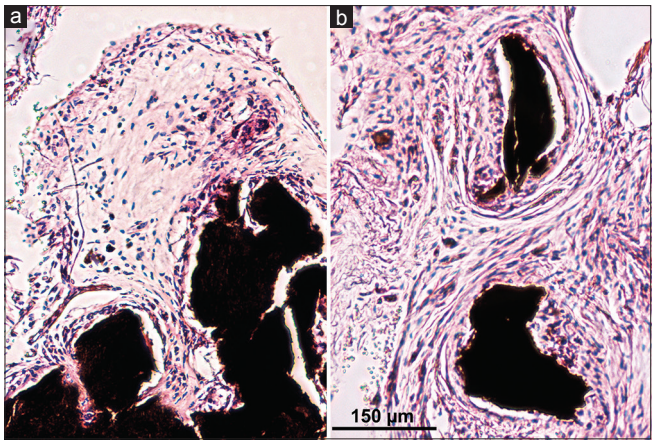

Figure 4: Representative phase contrast photomicrographs illustrate structural regeneration of spinal cord tissue using a nanoscaffold. The incompletely transected spinal cord is bridged using a reduced graphene oxide scaffold for tissue ingrowth and cell infiltration. (a), Spinal cord adheres well to the nanoscaffold. (b), Loose connective tissue forms between the spinal cord tissue and the reduced graphene oxide scaffold. Bar = 150 μm

nanoscaffold [Figure 3]. Neurofilaments were also seen in dense foci in proximity to the graphene nanoscaffold. This demonstrates that the graphene scaffold provides a favorable environment for the regeneration of neuronal elements. During axonal growth, new neurofilament subunits are incorporated along the length of the axon. Therefore, it is possible that local axonal sprouting and generation of neuritic processes occurred, which may have been directionally influenced and supported by the graphene nanoscaffold.

The presence of connective elements necessary for neuronal regeneration was detected around the graphene nanoscaffold. Chondroitin sulfate, stained with CS-56, was observed, with growth centered at the tissue-implant border [Figure 3]. Endothelial cells, stained with ED-1, were observed in close proximity to the graphene nanoscaffold [Figure 3]. Schwann cells, stained with p-75, were also found at the lesion site and in proximity to the graphene nanoscaffold, with diffuse growth throughout adjacent tissue [Figure 3].

Astrocytes, stained with GFAP-Cy3, were observed to have dense growth at the injury site, specifically bordering newly regenerated tissue around the graphene nanoscaffold [Figure 3]. This reactive astrocytosis, assumed to be a glial scar, serves as a barrier to neurite growth physically and through the upregulation of inhibitory molecules. The amount of glial scarring seen was expected. It was no different morphologically from the glial scar in the control group. In the presence of the glial scar, it appeared that the graphene nanoscaffold may have created a permissive environment for tissue regeneration [Figure 3].

The use of artificial implants in SCI raises concerns for possible inflammatory reactions toward the material. In our study, we observed cellular infiltration close to the graphene nanoscaffold of predominantly macrophages, as seen on H and E-stained sections and confirmed with ED-1 immunohistochemical stains, along with a few lymphocytes.

Combining scaffold implantation with the use of neurotrophic factors or stem cell treatment may lead to improved results. Loh *et al.*[38] found that modifying HPMA-RGD hydrogel with either BDNF or ciliary neurotrophic factor significantly increases the ingrowth of axons into the implant compared with results achieved with unmodified hydrogels. Other potential chemical/molecular pairings with graphene nanoscaffolds may prove effective, which could be explored in future research, including biofunctionalization with DNA and/or proteins.[62]

Our work to date has determined that graphene-based nanomaterials represent an additional promising group of bioscaffolds with potential to further advance SCI research. These nanoscaffolds have previously been shown to be biocompatible *in vitro*;[48] we have since demonstrated its biocompatibility in an *in vivo* SCI model. Moreover, we found a pronounced ingrowth of connective tissue and nervous tissue elements, such as NF 160–positive neurofilaments and Schwann cell projections, both in and adjacent to the reduced GO nanoscaffolds.

Limitations

Our study was qualitative in nature rather than quantitative. For example, because of artifact from tissue fixation and processing, we were unable to quantitatively evaluate the size of the perilesional pseudocyst in any experimental cohort. A qualitative study has many strengths: Playing an important role in suggesting possible relationships, causes, effects, and dynamic processes; examining forms of knowledge that otherwise might be unavailable through statistical analysis, thereby gaining new insight; and adding "flesh and blood" to the analysis of clinical implications. Nonetheless, qualitative research has significant drawbacks. The problem of adequate validity or reliability is a major criticism. Because of the subjective nature of qualitative data and its origin in single contexts, it is difficult to apply conventional standards of reliability and validity. Contexts, situations, events, conditions, and interactions cannot be replicated to any extent, nor can generalizations be made to a wider context other than the one studied with any confidence. In future study iterations, our methodology will include ways to quantitatively assess our data, including that contained in Figures 3 and 4.

Furthermore, our methodology did not include Luxol fast blue staining to evaluate the preserved gray and white matter and the perilesional cavity regions or GAP43 to show axonal elongation. A number of

immunostaining methods could have been used; however, there is precedent[27] for the staining techniques that we employed. Our study was a proof-of-principle that shows the feasibility and safety of placing 3D graphene in an animal model of SCI. We did not aim to show axonal regeneration; we only demonstrated that a favorable environment was present in the area around the graphene scaffolds for regeneration to occur. To show axonal regeneration, more sophisticated immunohistochemical staining would need to be performed.

Another weakness of our analysis is that we did not assess functional outcomes in our control and experimental animals. This deficiency will represent an arm of our investigation in future studies in both hemispinal and complete spinal cord transection models.

CONCLUSIONS

Our study showed the biocompatibility of an immobilized graphene-structured surface for direct neuronal interface *in vivo*. The 3D structure of reduced GO hydrogel allowed the growth of blood vessels, neurofilaments, and Schwann cells on its surface. Given its low toxicity when compared with other nanomaterials, graphene has significant potential as a key material in neuronal interface studies. Graphene's ability to carry neuroregenerative biomolecules, electrical conductivity, and neurocompatibility suggest the need for further investigation as a nanoscaffold in the treatment of SCI.

Financial support and sponsorship
Nil.

Conflicts of interest
There are no conflicts of interest.

REFERENCES

1. Agarwal S, Zhou X, Ye F, He Q, Chen GC, Soo J, *et al*. Interfacing live cells with nanocarbon substrates. Langmuir 2010;26:2244-7.
2. Allen MJ, Tung VC, Kaner RB. Honeycomb carbon: A review of graphene. Chem Rev 2010;110:132-45.
3. Altinova H, Mollers S, Fuhrmann T, Deumens R, Bozkurt A, Heschel I, *et al*. Functional improvement following implantation of a microstructured, type-I collagen scaffold into experimental injuries of the adult rat spinal cord. Brain Res 2014;1585:37-50.
4. Amr SM, Gouda A, Koptan WT, Galal AA, Abdel-Fattah DS, Rashed LA, *et al*. Bridging defects in chronic spinal cord injury using peripheral nerve grafts combined with a chitosan-laminin scaffold and enhancing regeneration through them by co-transplantation with bone-marrow-derived mesenchymal stem cells: Case series of 14 patients. J Spinal Cord Med 2014;37:54-71.
5. Anderson MA, Burda JE, Ren Y, Ao Y, O'Shea TM, Kawaguchi R, *et al*. Astrocyte scar formation aids central nervous system axon regeneration. Nature 2016;532:195-200.
6. Balandin AA, Ghosh S, Bao W, Calizo I, Teweldebrhan D, Miao F, *et al*. Superior thermal conductivity of single-layer graphene. Nano Lett 2008;8:902-7.
7. Berry M, Maxwell WL, Logan A, Mathewson A, McConnell P, Ashhurst DE, *et al*. Deposition of scar tissue in the central nervous system. Acta Neurochir Suppl 1983;32:31-53.
8. Bracken MB, Shepard MJ, Collins WF, Holford TR, Young W, Baskin DS, *et al*. A randomized, controlled trial of methylprednisolone or naloxone in the treatment of acute spinal-cord injury. Results of the Second National Acute Spinal Cord Injury Study. N Engl J Med 1990;322:1405-11.
9. Bracken MB, Shepard MJ, Collins WF, Jr., Holford TR, Baskin DS, Eisenberg HM, *et al*. Methylprednisolone or naloxone treatment after acute spinal cord injury: 1-year follow-up data. Results of the second National Acute Spinal Cord Injury Study. J Neurosurg 1992;76:23-31.
10. Bracken MB, Shepard MJ, Hellenbrand KG, Collins WF, Leo LS, Freeman DF, *et al*. Methylprednisolone and neurological function 1 year after spinal cord injury. Results of the National Acute Spinal Cord Injury Study. J Neurosurg 1985;63:704-13.
11. Bracken MB, Shepard MJ, Holford TR, Leo-Summers L, Aldrich EF, Fazl M, *et al*. Administration of methylprednisolone for 24 or 48 hours or tirilazad mesylate for 48 hours in the treatment of acute spinal cord injury. Results of the Third National Acute Spinal Cord Injury Randomized Controlled Trial. National Acute Spinal Cord Injury Study. JAMA 1997;277:1597-604.
12. Canavero S, Ren X, Kim CY, Rosati E. Neurologic foundations of spinal cord fusion (GEMINI). Surgery 2016;160:11-9.
13. Castro EV, Novoselov KS, Morozov SV, Peres NM, dos Santos JM, Nilsson J, *et al*. Biased bilayer graphene: Semiconductor with a gap tunable by the electric field effect. Phys Rev Lett 2007;99:216802.
14. Chen B, He J, Yang H, Zhang Q, Zhang L, Zhang X, *et al*. Repair of spinal cord injury by implantation of bFGF-incorporated HEMA-MOETACL hydrogel in rats. Sci Rep 2015;5:9017.
15. Chen J, Zhang Z, Liu J, Zhou R, Zheng X, Chen T, *et al*. Acellular spinal cord scaffold seeded with bone marrow stromal cells protects tissue and promotes functional recovery in spinal cord-injured rats. J Neurosci Res 2014;92:307-7.
16. Chen W, Yan L. *In situ* self-assembly of mild chemical reduction graphene for three-dimensional architectures. Nanoscale 2011;3:3132-7.
17. Chung YG, Algarrahi K, Franck D, Tu DD, Adam RM, Kaplan DL, *et al*. The use of bi-layer silk fibroin scaffolds and small intestinal submucosa matrices to support bladder tissue regeneration in a rat model of spinal cord injury. Biomaterials 2014;35:7452-9.
18. Du BL, Zeng X, Ma YH, Lai BQ, Wang JM, Ling EA, *et al*. Graft of the gelatin sponge scaffold containing genetically-modified neural stem cells promotes cell differentiation, axon regeneration, and functional recovery in rat with spinal cord transection. J Biomed Mater Res A 2015;103:1533-45.
19. Fehlings MG, Vaccaro A, Wilson JR, Singh A, D WC, Harrop JS, *et al*. Early versus delayed decompression for traumatic cervical spinal cord injury: Results of the Surgical Timing in Acute Spinal Cord Injury Study (STASCIS). PLoS One 2012;7:e32037.
20. Gao M, Lu P, Bednark B, Lynam D, Conner JM, Sakamoto J, *et al*. Templated agarose scaffolds for the support of motor axon regeneration into sites of complete spinal cord transection. Biomaterials 2013;34:1529-36.
21. Geim AK. Graphene: Status and prospects. Science 2009;324:1530-4.
22. Geim AK, Novoselov KS. The rise of graphene. Nat Mater 2007;6:183-91.
23. Hakim JS, Esmaeili Rad M, Grahn PJ, Chen B, Knight AM, Schmeichel AM, *et al*. Positively charged oligo[poly (ethylene glycol) fumarate] scaffold implantation results in a permissive lesion environment after spinal cord injury in rat. Tissue Eng Part A 2015;21:2099-114.
24. Han MY, Ozyilmaz B, Zhang Y, Kim P. Energy band-gap engineering of graphene nanoribbons. Phys Rev Lett 2007;98:206805.
25. Han S, Wang B, Jin W, Xiao Z, Chen B, Xiao H, *et al*. The collagen scaffold with collagen binding BDNF enhances functional recovery by facilitating peripheral nerve infiltrating and ingrowth in canine complete spinal cord transection. Spinal Cord 2014;52:867-73.
26. Han S, Wang B, Jin W, Xiao Z, Li X, Ding W, *et al*. The linear-ordered collagen scaffold-BDNF complex significantly promotes functional recovery after completely transected spinal cord injury in canine. Biomaterials 2015;41:89-96.
27. Hejcl A, Urdzikova L, Sedy J, Lesny P, Pradny M, Michalek J, *et al*. Acute and delayed implantation of positively charged 2-hydroxyethyl methacrylate scaffolds in spinal cord injury in the rat. J Neurosurg Spine 2008;8:67-73.
28. Jea A, Benglis DM, Falcone S, Green BA. Post-Traumatic Syringomyelia. In: Herkowitz G, Eismont, Bell, Balderston, editors. Rothman and Simeone's Spine Trauma, 2nd ed: The American Academy of Orthopedic Surgeons; 2011. p. 701-18.
29. Jian R, Yixu Y, Sheyu L, Jianhong S, Yaohua Y, Xing S, *et al*. Repair of spinal cord injury by chitosan scaffold with glioma ECM and SB216763 implantation in

adult rats. J Biomed Mater Res A 2015;103:3259-72.
30. Kaneko A, Matsushita A, Sankai Y. A 3D nanofibrous hydrogel and collagen sponge scaffold promotes locomotor functional recovery, spinal repair, and neuronal regeneration after complete transection of the spinal cord in adult rats. Biomed Mater 2015;10:015008.
31. Kim CY. PEG-assisted reconstruction of the cervical spinal cord in rats: Effects on motor conduction at 1 h. Spinal Cord 2016 [Epub ahead of print].
32. Koffler J, Samara RF, Rosenzweig ES. Using templated agarose scaffolds to promote axon regeneration through sites of spinal cord injury. Methods Mol Biol 2014;1162:157-65.
33. Lai BQ, Wang JM, Ling EA, Wu JL, Zeng YS. Graft of a tissue-engineered neural scaffold serves as a promising strategy to restore myelination after rat spinal cord transection. Stem Cells Dev 2014;23:910-21.
34. Li X, Yang Z, Zhang A, Wang T, Chen W. Repair of thoracic spinal cord injury by chitosan tube implantation in adult rats. Biomaterials 2009;30:1121-32.
35. Lim HN, Huang NM, Lim SS, Harrison I, Chia CH. Fabrication and characterization of graphene hydrogel via hydrothermal approach as a scaffold for preliminary study of cell growth. Int J Nanomedicine 2011;6:1817-23.
36. Liu C, Huang Y, Pang M, Yang Y, Li S, Liu L, *et al*. Tissue-engineered regeneration of completely transected spinal cord using induced neural stem cells and gelatin-electrospun poly (lactide-co-glycolide)/polyethylene glycol scaffolds. PloS One 2015;10:e0117709.
37. Liu Z, Robinson JT, Sun X, Dai H. PEGylated nanographene oxide for delivery of water-insoluble cancer drugs. J Am Chem Soc 2008;130:10876-7.
38. Loh NK, Woerly S, Bunt SM, Wilton SD, Harvey AR. The regrowth of axons within tissue defects in the CNS is promoted by implanted hydrogel matrices that contain BDNF and CNTF producing fibroblasts. Exp Neurol 2001;170:72-84.
39. Madigan NN, Chen BK, Knight AM, Rooney GE, Sweeney E, Kinnavane L, *et al*. Comparison of cellular architecture, axonal growth, and blood vessel formation through cell-loaded polymer scaffolds in the transected rat spinal cord. Tissue Eng Part A 2014;20:2985-97.
40. Madigan NN, McMahon S, O'Brien T, Yaszemski MJ, Windebank AJ. Current tissue engineering and novel therapeutic approaches to axonal regeneration following spinal cord injury using polymer scaffolds. Respir Physiol Neurobiol 2009;169:183-99.
41. Marcano DC, Kosynkin DV, Berlin JM, Sinitskii A, Sun Z, Slesarev A, *et al*. Improved synthesis of graphene oxide. ACS Nano 2010;4:4806-14.
42. Moore MJ, Friedman JA, Lewellyn EB, Mantila SM, Krych AJ, Ameenuddin S, *et al*. Multiple-channel scaffolds to promote spinal cord axon regeneration. Biomaterials 2006;27:419-29.
43. Myung S, Solanki A, Kim C, Park J, Kim KS, Lee KB. Graphene-encapsulated nanoparticle-based biosensor for the selective detection of cancer biomarkers. Adv Mater 2011;23:2221-5.
44. Novoselov KS, Geim AK, Morozov SV, Jiang D, Katsnelson MI, Grigorieva IV, *et al*. Two-dimensional gas of massless Dirac fermions in graphene. Nature 2005;438:197-200.
45. Novoselov KS, Geim AK, Morozov SV, Jiang D, Zhang Y, Dubonos SV, *et al*. Electric field effect in atomically thin carbon films. Science 2004;306:666-9.
46. Olson HE, Rooney GE, Gross L, Nesbitt JJ, Galvin KE, Knight A, *et al*. Neural stem cell- and Schwann cell-loaded biodegradable polymer scaffolds support axonal regeneration in the transected spinal cord. Tissue Eng Part A 2009;15:1797-805.
47. Rajnicek AM, Robinson KR, McCaig CD. The direction of neurite growth in a weak DC electric field depends on the substratum: Contributions of adhesivity and net surface charge. Dev Biol 1998;203:412-23.
48. Sahni D, Jea A, Mata JA, Marcano DC, Sivaganesan A, Berlin JM, *et al*. Biocompatibility of pristine graphene for neuronal interface. J Neurosurg Pediatr 2013;11:575-83.
49. Shapiro S, Borgens R, Pascuzzi R, Roos K, Groff M, Purvines S, *et al*. Oscillating field stimulation for complete spinal cord injury in humans: A phase 1 trial. J Neurosurg Spine 2005;2:3-10.
50. Sheng K, Xu Y, Li C, Shi G. High-performance self-assembled graphene hydrogels prepared by chemical reduction of graphene oxide. New Carbon Mater 2011;26:9-15.
51. Shi Q, Gao W, Han X, Zhu X, Sun J, Xie F, *et al*. Collagen scaffolds modified with collagen-binding bFGF promotes the neural regeneration in a rat hemisected spinal cord injury model. Sci China Life Sci 2014;57:232-40.
52. Shrestha B, Coykendall K, Li Y, Moon A, Priyadarshani P, Yao L. Repair of injured spinal cord using biomaterial scaffolds and stem cells. Stem Cell Res Ther 2014;5:91.
53. Sisken BF, Walker J, Orgel M. Prospects on clinical applications of electrical stimulation for nerve regeneration. J Cell Biochem 1993;51:404-9.
54. Spilker MH, Yannas IV, Kostyk SK, Norregaard TV, Hsu HP, Spector M. The effects of tubulation on healing and scar formation after transection of the adult rat spinal cord. Restor Neurol Neurosci 2001;18:23-38.
55. Stankovich S, Dikin DA, Dommett GH, Kohlhaas KM, Zimney EJ, Stach EA, *et al*. Graphene-based composite materials. Nature 2006;442:282-6.
56. Stokols S, Tuszynski MH. Freeze-dried agarose scaffolds with uniaxial channels stimulate and guide linear axonal growth following spinal cord injury. Biomaterials 2006;27:443-51.
57. Sui Z, Zhang X, Lei Y, Luo Y. Easy and green synthesis of reduced graphite oxide-based hydrogels. Carbon 2011;49:4314-21.
58. Sun Y, Wu Q, Shi G. Supercapacitors based on self-assembled graphene organogel. Phys Chem Chem Phys 2011;13:17249-54.
59. Ukegawa M, Bhatt K, Hirai T, Kaburagi H, Sotome S, Wakabayashi Y, *et al*. Bone marrow stromal cells combined with a honeycomb collagen sponge facilitate neurite elongation *in vitro* and neural restoration in the hemisected rat spinal cord. Cell Transplant 2015;24:1283-97.
60. Vale FL, Burns J, Jackson AB, Hadley MN. Combined medical and surgical treatment after acute spinal cord injury: Results of a prospective pilot study to assess the merits of aggressive medical resuscitation and blood pressure management. J Neurosurg 1997;87:239-46.
61. Wang D, Liang J, Zhang J, Liu S, Sun W. Mild hypothermia combined with a scaffold of NgR-silenced neural stem cells/Schwann cells to treat spinal cord injury. Neural Regen Res 2014;9:2189-96.
62. Wang Y, Li Z, Wang J, Li J, Lin Y. Graphene and graphene oxide: Biofunctionalization and applications in biotechnology. Trends Biotechnol 2011;29:205-12.
63. Watcharotone S, Dikin DA, Stankovich S, Piner R, Jung I, Dommett GH, *et al*. Graphene-silica composite thin films as transparent conductors. Nano Lett 2007;7:1888-92.
64. Wu C, Zhou Y, Miao X, Ling L. A novel fluorescent biosensor for sequence-specific recognition of double-stranded DNA with the platform of graphene oxide. Analyst 2011;136:2106-10.
65. Xu Y, Sheng K, Li C, Shi G. Self-assembled graphene hydrogel via a one-step hydrothermal process. ACS Nano 2010;4:4324-30.
66. Ye Y, Kim CY, Miao Q, Ren X. Fusogen-assisted rapid reconstitution of anatomophysiologic continuity of the transected spianl cord. Surgery 2016;160:20-5.
67. Yoshii S, Ito S, Shima M, Taniguchi A, Akagi M. Functional restoration of rabbit spinal cord using collagen-filament scaffold. J Tissue Eng Regen Med 2009;3:19-25.
68. Zhang L, Shi G. Preparation of Highly Conductive Graphene Hydrogels for Fabricating Supercapacitors with High Rate Capability. J Phys Chem C 2011;115:17206-12.
69. Zhang Y, Ali SF, Dervishi E, Xu Y, Li Z, Casciano D, *et al*. Cytotoxicity effects of graphene and single-wall carbon nanotubes in neural phaeochromocytoma-derived PC12 cells. ACS Nano 2010;4:3181-6.